FULL PAPER

Dalton
www.rsc.org/dalton

A new bis(3-hydroxy-4-pyridinone)-IDA derivative as a potential therapeutic chelating agent. Synthesis, metal-complexation and biological assays

M. Amélia Santos,*[a] Sofia Gama,[a] Lurdes Gano,[b] Guilhermina Cantinho[c] and Etelka Farkas[d]

[a] *Centro de Química Estrutural, Instituto Superior Técnico, Complexo I, 1049-001 Lisboa, Portugal. E-mail: masantos@ist.utl.pt; Fax: +351 21 846 44 55; Tel: +351 218419273*

[b] *Instituto Tecnológico e Nuclear, Estrada Nacional N° 10, 2686-953 Sacavém, Portugal*

[c] *Instituto de Medicina Nuclear, Faculdade de Medicina de Lisboa, R. Egas Moniz, 1600 Lisboa, Portugal*

[d] *Department of Inorganic and Analytical Chemistry, University of Debrecen, H-4010 Debrecen, Hungary*

Received 21st June 2004, Accepted 24th September 2004
First published as an Advance Article on the web 12th October 2004

A new bis(3-hydroxy-4-pyridinone) derivative of iminodiacetic acid, imino-bis(acetyl(1-(3′-aminopropyl)-3-hydroxy-2-methyl-4-pyridinone)), IDAPr(3,4-HP)$_2$, has been prepared and studied in its interaction with a set of hard metal ions. This tetradentate ligand presents a much higher chelating efficiency for trivalent hard metal ions (Fe, Ga, Al) than the monodentate derivative Deferriprone, namely at the diluted conditions prevailing in physiological conditions and at low clinical doses. A similar behaviour was also observed for the complexation with Zn(II) but at a significantly lower extent. This compound presents a moderate hydrophilic character at physiological pH (log$D$ = −1.72). *In vivo* assays showed much more rapid clearance of ^{67}Ga from most tissues of metal-loaded mice than the drug Deferriprone and the radioactivity excretion occurs mostly through the kidneys. Therefore, results from *in vitro* and *in vivo* studies indicated good perspectives for this compound to be a potential decorporating agent for hard metal ions in overload situations without depletion of essential metal ions such as zinc.

Introduction

The relevance of specific metal chelators in medicine has increased in recent years, namely compounds with high affinity towards "hard" M^{3+} metal ions such as iron and the group 13 metals (aluminium, gallium and indium), due to their potential application, either for controlling situations of metal toxicity in the body (*e.g.* Fe, Al) or for clinical diagnosis and chemotherapy (*e.g.* ^{67,68}Ga, ^{111}In). The 3-hydroxy-4-pyridinones (3,4-HP), having a hydroxy group *ortho* to a ketone functionality, are a class of hydroxypyridinones with high ability to complex metal cations with large charge/ionic radius ratios and they have been strongly suggested as good candidates for medicinal chemistry.[1–3] In particular, 1,2-dimethyl-3-hydroxy-4-pyridinone (3,4-DMHP, commercially available as Deferriprone) has already been clinically used as an orally active iron-chelating drug in thalassemic patients, in substitution of Desferrioxamine (DFO), the well established tris-hydroxamate derivative.[4] However, one important limitation to the clinical application of bidentate metal decorporating agents such as Deferriprone emerges from the great ligand concentration dependence of their chelating efficacy as compared to those of multidentate ligands, which can be used at much lower clinical doses. Therefore, in order to minimize drug-induced toxicity, considerable efforts have been made on the design of new ligands with high denticity and presumably high ability for formation of stable 1 : 1 (M : L) complexes with that type of metal ions.[1,3,5–8] However, most of the tris-hydroxypyridinones studied so far are of 3-hydroxy-2-pyridinone (3,2-HP) type, which are known to present less affinity for the hard metal ions at the physiological pH and to involve more laborious methods of synthesis than the corresponding 3,4-HP derivatives. On the other hand, polyaminocarboxylic compounds, such as ethylenediaminetetracetic acid (EDTA) and diethylenetriaminepentaacetic acid (DPTA), have good ability to form 1 : 1 complex with a large variety of metal ions and they are zwitterionic species with very good solubility properties. However, the lack of specificity of these compounds for metal-complexation limits their clinical applications for chelating therapy of hard metal ions, namely because they can also efficiently bind to other essential metal ions, notably zinc and calcium, causing their depletion *in vivo*.

As part of an ongoing project aimed at exploring the polydenticity of 3,4-HP derivatives, in addition to the development of tris-hydroxypyridinonates (hexadendate ligands),[9] we sought to explore tetradentate bis-hydroxypyridinone derivatives, having two 3,4-HP binding groups appended to various molecular scaffolds with the potential existence of extra-functional groups for molecular interaction with biological sites. Following this molecular-designing option, firstly we used a cyclohexane backbone with two 3,4-HP units and one carboxylate group as pendant arms [KEMPPr(3,4-HP)$_2$, see Chart 1]. Although this

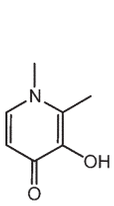

3,4-DMHP

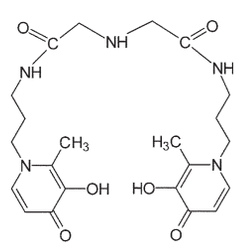

IDAPr(3,4-HP)$_2$

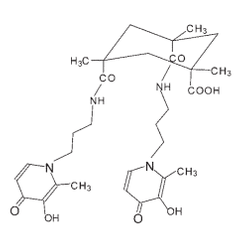

KEMPPr(3,4-HP)$_2$

Chart 1

DOI: 10.1039/b409357g

tetradentate ligand showed reasonably good ability to form 1 : 1 complexes with the set of M^{2+} and M^{3+} metal ions,[10,11] there was some apparent strain associated to the metal wrapping by the hydroxypyridone moieties and also water-solubility limitations. Therefore, we have decided to change the ligand topology by choosing another type of molecular scaffold, namely linear polyaminocarboxylic derivatives.

Herein we report the preparation of a new tetradentate derivative, IDAPr(3,4-HP)$_2$ (see Chart 1) which has the iminodiacetic acid (IDA) as molecular scaffold and two 3,4-HP binding groups attached to its carboxylic groups, thus leaving the amino group free for further potential interaction with biological sites or for appending other receptor probes. We examine its physico-chemical properties in aqueous solution, alone and in the presence of a set of metal ions, and also results of *in vivo* assays. In particular, equilibrium studies in aqueous solution, mostly based on potentiometric and spectroscopic (UV-Vis, ^{1}H NMR, ^{27}Al NMR) measurements, are conducted to investigate the binding affinities towards the proton and a set of trivalent (Fe, Ga, Al) metal ions, and also Zn(II) due to its availability in biological systems. Due to the great importance of the lipo/hydrophilic character of a drug for the assessment of its bioavailability, the distribution coefficient of IDAPr(3,4-HP)$_2$ between 1-octanol and a Tris buffered (pH 7.4) aqueous solution is also calculated. The ability of the new chelating agent to mobilize ^{67}Ga from radiotracer overloaded mice and the biodistribution of the ^{67}Ga-IDAPr(3,4-HP)$_2$ complex is further assayed to evaluate potential pharmaceutical applications of this new bis(3-hydroxy-4-pyridinone) compound, in comparison with Deferriprone.

Experimental

Materials

Analytical grade reagents were used as supplied. Whenever necessary, solvents were dried according to standard methods.[12] All the chemical reactions were TCL controlled.

Synthesis of the ligand

3-Benzyloxy-2-methyl-4-pyrone. To a solution of 3-hydroxy-2-methyl-4-pyrone (10.00 g; 79 mmol) containing the equivalent amount of a 7 M NaOH aqueous solution (12 mL) in methanol (100 mL), benzyl chloride (10.6 mL; 92 mmol) was dropwise added and the mixture was left to reflux for 6 h. After cooling, the reaction mixture was filtered and the filtrate was evaporated under vacuum. The residual oil was taken in dichloromethane (50 mL) and washed with 5% NaOH aqueous solution (5 × 20 mL) and finally with water. The organic solution was dried with anhydrous sodium sulfate and the solvent was evaporated to dryness to obtain the pure product as a pale oil (η = 85%). ^{1}H NMR ($CDCl_3$) δ (ppm): 7.57 (1H, d, 6-*H*Py); 7.32 (5H, s, Ph); 6.33 (1H, d, 5-*H*Py); 5.14 (2H, s, C*H*$_2$Ph); 2.06 (s, 3H, C*H*$_3$). *m*/*z* (FAB-MS): 217 (M + 1).

(3′-Aminopropyl)-3-benzyloxy-2-methyl-4-pyridinone. 3-Benzyloxy-2-methyl-4-pyrone (9.37 g, 43.59 mmol) and 1,3-diaminopropane (3.8 mL, 45.6 mmol) were left refluxing (T = 70–75 °C), in a EtOH–water mixture (20/15) mL with 2 M NaOH (4 mL) for 24 h. After cooling, 2 M HCl was added until *ca*. pH = 1 and the ethanol was evaporated. To the remaining residue, water was added (50 mL) and this solution was extracted with ether (2 × 50 mL). The aqueous phase was basified with 10 M NaOH until pH ≈ 12 and then it extracted with dichloromethane (5 × 50 mL). The organic solution was dried over anhydrous sodium sulfate and the solvent was evaporated to dryness. That residue was taken into methanol (2 mL). Acidification of that solution until *ca*. pH 1 with HCl-saturated methanol gave a white precipitate which was recrystallized from dry methanol–acetonitrile to give the pure product as the corresponding hydrochloride salt (η = 40%), mp 186–189 °C. ^{1}H NMR ($CDCl_3$) δ (ppm): 8.14 (1H, d, 6-*H*Py), 7.42 (5H, s, Ph), 7.11 (1H, d, 5-*H*Py), 5.13 (2H, s, C*H*$_2$Ph), 4.31 (2H, t, C*H*$_2$NPy), 3.03 (2H, t, C*H*$_2$NH$_2$), 2.36 (2H, t, CH$_2$C*H*$_2$CH$_2$), 2.12 (3H, s, C*H*$_3$). *m*/*z* (FAB-MS) 273 (M + 1).

***N*-Benzylimino-bis(acetyl(1-(3′-aminopropyl)-3-benzyloxy-2-methyl-4-pyridinone)).** Free 1-(3′-aminopropyl)-3-benzyloxy-2-methyl-4-pyridinone was obtained by adding a solution of KOH (525 mg, 9.36 mmol) in dry methanol (5 mL) to a solution of 1-(3′-aminopropyl)-3-benzyloxy-2-methyl-4-pyridinone hydrochloride (1.45 g, 4.68 mmol) in dry methanol (20 mL), under nitrogen, in a water-ice bath. The mixture was allowed to stir for 15 min and then KCl was filtered out. In a two-neck round flask, *N*-benzyliminodiacetic acid (494 mg, 2.21 mmol) was dissolved in dry THF (50 mL) and the solution was kept under nitrogen at *ca*. 0 °C. Then, *N*-methylmorpholine (495 mg, 4.89 mmol) and ethylchloroformate (579 mg, 5.34 mmol) were added, the mixture was left under stirring for 2 h and the *N*-methylmorpholine hydrochloride salt was filtered out. To this solution, the free 1-(3′-aminopropyl)-3-benzyloxy-2-methyl-4-pyridinone solution was dropwise added under stirring and the solution was allowed to stir for 3.5 h keeping the temperature at *ca*. 0 °C. The solution was filtered and the solvent was removed in vacuum. The solid residue was purified by flash chromatography on a silica-gel column. The isolated product was recrystallized from dry methanol–ether (η = 45%). ^{1}H NMR ($CDCl_3$) δ (ppm): 8.70 (2H, d, 6-*H*Py), 7.3 (15H, s, Ph), 6.29 (2H, d, 5-*H*Py), 5.09 (4H, s, OC*H*$_2$Ph), 3.80 (4H, t, NC*H*$_2$CH$_2$CH$_2$NHCO), 3.67 (2H, s, NC*H*$_2$Ph), 3.20 (6H, s, C*H*$_3$), 2.12–2.02 (4H + 4H, m, C*H*$_2$NHCO + COC*H*$_2$NC*H*$_2$CO), 1.79 (4H, t, CH$_2$C*H*$_2$CH$_2$). *m*/*z* (FAB-MS): 732 (M + 1).

Imino-bis(acetyl(1-(3′-aminopropyl)-3-hydroxy-2-methyl-4-pyridinone)). To a solution of *N*-benzylimino-bis(acetyl(1-(3′-aminopropyl)-3-benzyloxi-2-methyl-4-pyridinone)) (837 mg, 1.14 mmol) in dry methanol (10 mL) was added 10% Pd/C (282 mg) and the mixture was stirred under H_2 (1.5 atm) for 4 h, at room temperature. After filtration, the solvent was evaporated under reduced pressure and the product (489 mg) was obtained as a white powder, which was recrystallised from methanol–ether (η = 93%), mp 95–97 °C. ^{1}H NMR ($CDCl_3$) δ (ppm): 7.67 (2H, d, 6-*H*Py), 6.53 (2H, d, 5-*H*Py), 4.14 (4H, t, NC*H*$_2$CH$_2$CH$_2$NHCO), 3.32 (4H + 4H, m, C*H*$_2$NHCO + COC*H*$_2$NHC*H*$_2$CO), 2.43 (6H, s, C*H*$_3$), 2.03 (4H, t, CH$_2$C*H*$_2$CH$_2$). *m*/*z* (FAB-MS): 462 (M + 1). Calc. for $C_{22}N_5H_{31}O_6\cdot 3H_2O\cdot 0.8$ MeOH: C, 52.38; H, 7.78; N, 12.94. Found: C, 52.60; H, 7.31; N, 12.68%.

Potentiometric measurements

The potentiometric measurements were performed with a Metrohm 6.0234.100 combined electrode and a Dosimat 765 burette controlled by computer, at T = 25 ± 0.1 °C and I = 0.1 M (KNO_3), using a CRISON emf-Meter. Measuring the emf in the cell, [H$^+$] of the solutions was calculated taking into account that $E = E°' + Q\log[H^+] + E_j$. $E°'$ and Q were obtained daily by calibration of the electrode applying Gran's method[13] to a strong acid/strong base (HNO_3/KOH 0.1 M) titration in the acid range at the same ionic strange, and E_j has a negligible value at the used experimental conditions. The K_w value used in the calculations was $10^{-13.78}$ and it was also determined from a strong acid/strong base titration using the alkaline range data. Atmospheric CO_2 was excluded from the system with a purging stream of N_2. The ligand (H_2L) concentration in the sample was 1.75×10^{-3} M. The exact concentration of the ligand stock solution and the protonation constants was determined from the fitting analysis of the potentiometric data with the HYPERQUAD 2000 computer program.[14] Complexation studies were performed for each metal ion by potentiometric titrations with the same computer program, although in some cases combined with spectrophotometric measurements (see below). To study the formation of the species with 1 : 1 and the

2 : 3 stoichiometries, 1 : 1 and 1 : 2 metal ion-to-ligand ratios were used, respectively. Since the 2 : 3 species is supposed to be formed at a higher pH than the 1 : 1 species, in that case, a ligand excess was used to suppress hypothetical precipitation due to hydrolytic species. The metal ions were provided from stock solutions of the corresponding nitrate salts.

The selection of the equilibrium models was based on the critical analysis of the weighted residuals, the statistical parameters (χ^2, σ)[15] and graphical comparisons between the experimental and simulated potentiometric curves.

Spectrophotometric measurements

Spectral determinations were made with a Perkin-Elmer Lambda 9 spectrophotometer using 1.0 cm matched quartz cells at T = 25.0 °C and constant ionic strength conditions. Solutions of the metal complexes were generated *in situ* by addition of a standard metal ion solution to the ligand solution. The pH values were measured using a Crison emf-Meter equipped with a Metrohm 6.0234.100 combined electrode. For very acidic conditions (pH < 2), the stability constants of the corresponding iron(III) and gallium(III) complexes were calculated from the spectrophotometric data, using the PSEQUAD program,[16] and the fitting parameter accepted was below 2×10^{-2}.

Distribution coefficients

The distribution coefficient of the ligand in octanol/water (Tris buffered solution, pH = 7.4) at *ca.* 25 °C was determined by the "shakeflask" method, as previously described[17] and based on established procedures.[18] The ligand concentrations were evaluated by UV spectrophotometry, measuring the absorbance of its benzenoid bands (π–π^*) at λ = 280 nm. The distribution coefficients, D (or log$D$), were obtained as the ratio of the ligand concentrations in the organic phase to that in the aqueous phase.

Biodistribution studies

Animal experiments were carried out with groups of 3–5 female mice CD-1 (randomly bred Charles River, from CRIFFA, Spain) weighing approximately 25 g. Animals were intravenously injected with 100 μL (5–10 MBq) of ^{67}Ga-citrate *via* the tail vein (Group 1). A separated group of animals was simultaneously intraperitoneally injected with 0.5 μmol of the ligand in 100 μL saline solution (Group 2). A third group was intraperitoneally injected with 0.5 μmol of the ligand in 100 μL saline solution, 30 min after the administration of ^{67}Ga-citrate (Group 3). Finally, another group was intravenously injected with 100 μL (5–10 MBq) of the ^{67}Ga-complex previously prepared (Group 4). Mice were maintained on normal diet *ad libitum.* At 5 min, 15 min, 30 min, 1 h, 24 h and 48 h post-administration, animals were killed by cervical dislocation. The radioactive dosage administered and the radioactivity in the sacrificed animal were determined by counting in a dose calibrator (Aloka, Curiemeter IGC-3, Aloka, Tokyo, Japan). The difference between the radioactivity in the injected and the sacrificed animal was assumed to be due to excretion. Tissue samples of main organs were then removed for counting in a gamma counter (Berthold LB2111, Berthold Technologies, Germany). Biodistribution results were expressed as percent of injected dose per total organ (% ID/organ). For blood, bone and muscle, total activity was calculated assuming, as previously reported,[17] that these organs constitute 7, 10 and 40% of the total weight, respectively. However, the accuracy of these values is not very important because they are used to calculate the organ uptakes in all the experimental results which are then taken for comparison purposes.

Other measurements

^{1}H NMR spectra were recorded using a Varian Unity 300 spectrometer at 25 °C. The chemical shifts are reported in ppm (δ) from sodium 3-(trimethylsilyl)-[2,2,3,3-^{2}D$_4$]propionate (DSS) internal reference in D_2O solutions and tetramethylsilane (TMS) in organic solvents. Some abbreviations are used to characterize the peaks: d, doublet; s, singlet; t, triplet. Solution magnetic susceptibilities were measured in D_2O solution, as a function of pD,[19] by the Evans method[20] (χ_M, calculated per molar concentration of iron) and the corresponding magnetic moments were calculated ($\mu_M = 2.84(\chi_M T)^{1/2}$,[21] for both the Fe : L stoichiometries, under the same experimental conditions used for potentiometry, at T = 298 K. Melting points were measured using a Leica Galen III hot stage apparatus and they are uncorrected values. Elemental analysis was performed on a Fisons EA1108 CHNF/O instrument and the mass spectra results were recorded on a VG TRIO-2000 GC/MS instrument.

Results and discussion

Synthesis

This ligand was synthesized through a straightforward method outlined in Scheme 1. Two equivalents of 1-(3′-aminopropyl)-3-benzyloxy-2-methyl-4-pyridinone were condensed with *N*-benzyliminodiacetic acid, upon its previous activation with ethylchloroformate in THF. Purification by flash silica-gel chromatography column afforded the bis-hydroxypyridinone *N*,*O*-protected intermediate, IDABzPr(3,4-HPBz)$_2$, in 45% yield as a beige solid. Removal of the benzyl protecting groups was performed by standard hydrogenolysis (1.5 atm H_2 over 10% Pd/C) to give the final product, IDAPr(3,4-HP)$_2$, as a white powder (η = 93%).

Protonation

In its neutral form, the ligand [IDAPr(3,4-HP)$_2$, hereafter also designed as H_2L] has two dissociable protons, corresponding to the pyridinone hydroxy groups, but the fully protonated form of the ligand has three extra N–H protons associated to two pyridinium and one ammonium groups. The fitting analysis of the corresponding potentiometric titration curve (Fig. 1) by the HYPERQUAD 2000 program[14] gave the global protonation constants which allowed the calculation of the stepwise protonation constants (logK_i) presented in Table 1. For comparison purposes, this table also includes the protonation constants reported in the literature for the bidentate 1,2-dimethyl-3-hydroxy-4-pyridinone (3,4-DMHP).[22] Analysis of Table 1 shows that the calculated logK_i for IDAPr(3,4-HP)$_2$ are according to chemical evidences. In fact, the first two protonation constants (9.94, 9.44) are easily attributed to the hydroxypyridinone hydroxy groups and the third one (5.42) is attributed to the amine group, as suggested by its similarity with

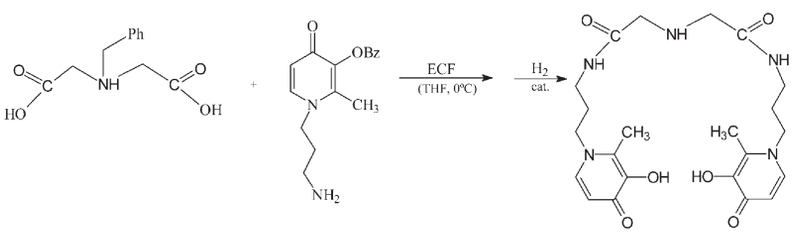

Scheme 1 Synthesis procedure for the ligand.

Table 1 Stepwise protonation constants for IDAPr(3,4-HP)$_2$ and DMHP; global formation constants (logβ) for their metal complexes (M = Fe, Ga, Al, Zn) at I = 0.1 M KNO_3 and 25.0 °C; pM values for these compounds and some relevant synthetic and biological ligands

Compound	logK_i	(p,q,r)	logβ $Fe_pH_qL_r$	$Ga_pH_qL_r$	$Al_pH_qL_r$	$Zn_pH_qL_r$
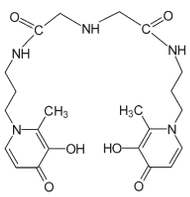 IDAPr(3,4-HP)$_2$		(2,−2,2)	44.00(9)	—	32.05(6)	
		(1,−1,1)	—	18.23(9)	—	
		(2,3, 3)	89.53(2)	84.97(1)	76.46(2)	
	9.94(1)	(2,2,3)	85.54(3)	80.16(4)	71.72(3)	
	9.44(1)	(2,1,3)	79.90(9)	74.64(4)	66.21(3)	
	5.42(2)	(2,0,3)	7426(6)	68.44(4)	60.18(3)	
	3.54(2)	(1,3,1)	33.59(2)	33.21(9)	30.44(6)	27.28(1)
	3.11(3)	(1,2,1)	—	—	27.71(5)	
		(1,1,1)	31.16(3)	28.83(7)	25.37(2)	18.92(6)
		(1,0,1)	26.16(4)	24.30(8)	20.35(3)	13.30(3)
		pM	**25.8**	**22.9**	**18.8**	**9.7**
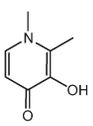		(1,0,1)	15.10	13.17	12.20	7.19
	9.77	(1,0,2)	26.61	25.43	23.25	13.53
	3.68	(1,0,3)	35.88	35.76	32.62	—
3,4-DMHP[a]		**pM**	**19.3**	**19.4**	**16.1**	**6.2**
KEMPPr(3,4-HP)$_2$[b]	—	**pM**	**20.5**	**18.8**	**18.1**	**9.5**
DTPA[c]	—	**pM**	**24.6**	**20.9**	**15.2**	**14.8**
DOTA[c]	—	**pM**	**24.3**	**18.8**	**13.2**	**17.9**
DBF[d]	—	**pM**	**26.5**	**22.4**	**19.3**	**6.6**
Transferrin	—	**pM**	**20.3**[e]	**20.3**[f]	**14.5**[g]	—

pM = −log[M] with C_L/C_M = 10 and C_M = 10^{-6} M. [a] Ref. 21. [b] Ref. 11. [c] Ref. 31. [d] Refs. 32 and 33. [e] Ref. 34. [f] Ref. 35. [g] Ref. 36.

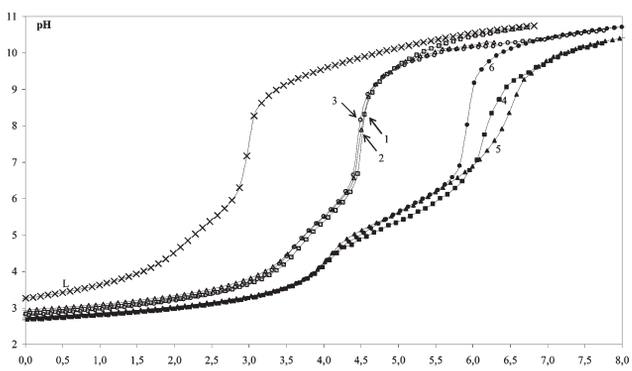

Fig. 1 Potentiometric titration curves of IDAPr(3,4-HP)$_2$, alone (C_L = 5.998 × 10^{-4} M) and in presence of the three-charged metal ions (M^{3+}), at conditions of: *ca.* 1:2 metal–ligand system molar ratio and C_{Fe} = 2.844 × 10^{-4} M (1), C_{Ga} = 2.982 × 10^{-4} M (2), C_{Al}= 2.972 × 10^{-4} M (3); *ca.* 1:1 metal–ligand ratio and C_{Fe} = 5.918 × 10^{-4} M (4), C_{Ga} = 5.540 × 10^{-4} M (5), C_{Al} = 5.631 × 10^{-4} M (6). T = 25.0 °C, I = 0.1 M, KNO_3).

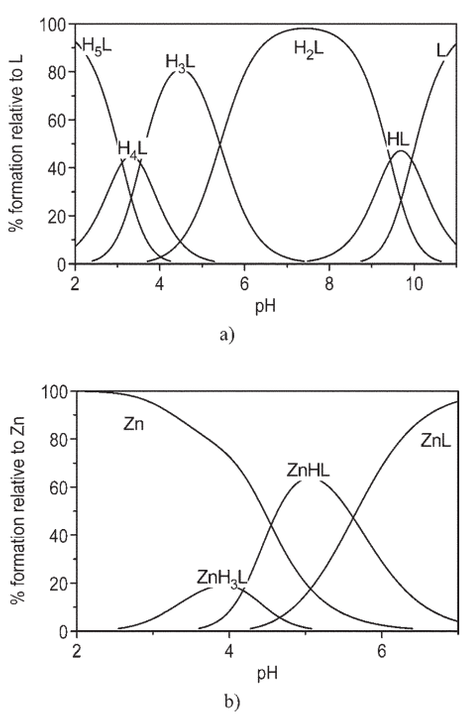

Fig. 2 Concentration distribution curves of the free ligand IDAPr(3,4-HP)$_2$ (C_L = 5.998 × 10^{-4} M) (a) and of the complexes formed in the system Zn(II)–IDAPr(3,4-HP)$_2$ at (1:1) metal to ligand ration, C_M = 1.8 × 10^{-3} M (b).

the corresponding value for iminodihydroxamic acid (IDHA, logK_1 = 5.66).[23] The fairly acidic character of this protonated amine group should be due to some electron-withdrawing effect of the amide groups in its vicinity as well as to some stabilization of the conjugated base by hydrogen bonding (amide –NH to N–amine) through the formation of stable five-membered rings. The two remaining protonation constants (logK_i = 3.54, 3.11) are undoubtedly attributed to pyridinium protons. Therefore, based on the calculated protonation constants, the neutral form of the ligand (H_2L) should be the major species at the physiological pH (Fig. 2(a)).

Metal complexation

Although the main interest of the present metal-complexation studies is centred on a set of three-charged hard metal ions with biological interest (Fe, Al, Ga), the fact that zinc is an essential element present in biological systems led us to make a preliminary evaluation of the interaction of this ligand with Zn(II) by potentiometry. Analysis of the potentiometric titration curve for the 1:1 metal-to-ligand ratio conditions showed that the complexation started only at pH ≈ 3.5 and the last deprotonation could not be completely finished because precipitation occurred (pH ≈ 7), probably due to formation of neutral species. The deprotonation of the ammonium group is not greatly affected by the presence of the metal ion, thus suggesting that the amine group is not involved in the coordination to the metal ion. The first species to be formed (ZnH_3L) has the metal ion coordinated by one hydroxypyridinone moiety (HP), thus keeping one amine and two HP protons (hydroxy and pyridinium). Therefore, when ZnH_3L releases both these HP protons (in a cooperative way) ZnHL is formed (two HP moieties are coordinated to the metal ion and the amine still remains protonated). A brief analysis of the global formation

constants ($\log\beta_{ML}$) calculated for the 1 : 1 (M : L) complexes with IDAPr(3,4-HP)$_2$ shows they are very close to the values obtained for the corresponding 1 : 2 complexes, $\log\beta_{ML_2}$, with the mono-hydroxypyridinone derivative (Deferriprone; Table 1), thus indicating identical hydroxypyridonate coordination mode. However, due to differences on the denticity and the acidity of these ligands, accurate comparison of their metal-complexation effectiveness is better based on the corresponding pM values (pM = −log[M^{2+}] for pH = 7.4 at micromolar concentration of the metal ion and 10-fold ligand excess), assuming that no precipitation takes place. Therefore, IDAPr(3,4-HP)$_2$ presents higher affinity for zinc than the corresponding mono-derivatives but it is still quite low (pZn = 9.7) and, at the physiological pH, the major complex species is in the neutral form (ZnL, Fig. 2).

To study the complexation behaviour of IDAPr(3,4-HP)$_2$ towards the M^{3+} hard metal ions (M = Fe, Al, Ga) in aqueous solutions, potentiometric and spectrophotometric techniques were used at various metal-to-ligand molar ratios. Representative potentiometric titration curves are shown in Fig. 1 for the ligand alone and in the presence of each of those M^{3+} metal ions, at the 1 : 2 and 1 : 1 metal-to-ligand molar ratios. For each of these binary systems there is a considerable drop of the pH at the beginning of the titration, thus indicating high affinity of the ligand for these metal ions. A more detailed analysis of the (1 : 1) titration curves shows the existence of breaks at a = 4 (a = mol of base per mol of the ligand), indicating that at *ca.* pH = 3.5 four protons have been released (presumably from two hydroxy and two pyridinium groups). Accordingly, there was formation of the MHL species, having the metal ion coordinated to both hydroxypyridinone moieties but the amine group being still protonated. However, analysis of the (1 : 1) titration curves showed that one extra deprotonation process is occurring (*ca.* one equivalent of extra base consumption), which should be due to some hydrolytic process. As expected, this process was not observed in the presence of ligand excess.

Fitting analysis of the potentiometric and spectrophotometric titration data, for each ligand–metal system at both the metal-to-ligand molar ratios, leads to a speciation model of the complex species whose global stability constants are listed in Table 1.

Spectrophotometric titrations of the IDAPr(3,4-HP)$_2$–Fe system with base were also performed, at both the stoichiometric conditions used for potentiometric measurements, to aid the understanding of the complexation model. Analysis the pH dependency of UV-Vis electronic spectra (Fig. 3) suggests the existence of different equilibrium models for each stoichiometric condition.

Spectrophotometric titrations further indicate that the complexation process starts at *ca.* pH 0.4. Therefore, at the beginning of the potentiometric titrations (*ca.* pH = 2), the complex formation was already complete. Therefore to study the stability constants of the corresponding species it was required to go to a lower pH and this study could not be performed by potentiometry because we could not measure the pH value. However, below pH 2, the pH could be accurately calculated based on the analytical concentration of the proton and the equilibrium process could be followed and studied by spectrophotometry. In fact, analysis of the spectrophotometric spectra (Fig. 3) shows that from the beginning of the titration (pH = 0.4), the formation of the monochelated and other species could be easily followed by the changes of the wavelength and absorbance values which are in agreement with the species distribution diagram. A detailed analysis of Fig. 3 indicates that the spectral parameters for the species with maximum concentration at *ca.* pH 1 (FeH_3L; λ_{max} = 562 nm, ε = 2079 M^{-1} cm^{-1}) and 1.8 (FeHL; λ_{max} = 510 nm, ε = 3593 M^{-1} cm^{-1}) correspond to the CT absorption bands of mono- and bis-chelated species, respectively, in agreement with literature reports for Fe(III)–(3-hydroxy-4-pyridinone) complexes.[22] Above this pH value, both the stoichiometric systems presented blue-shifts of the absorption bands, thus indicating further increase of the degree of

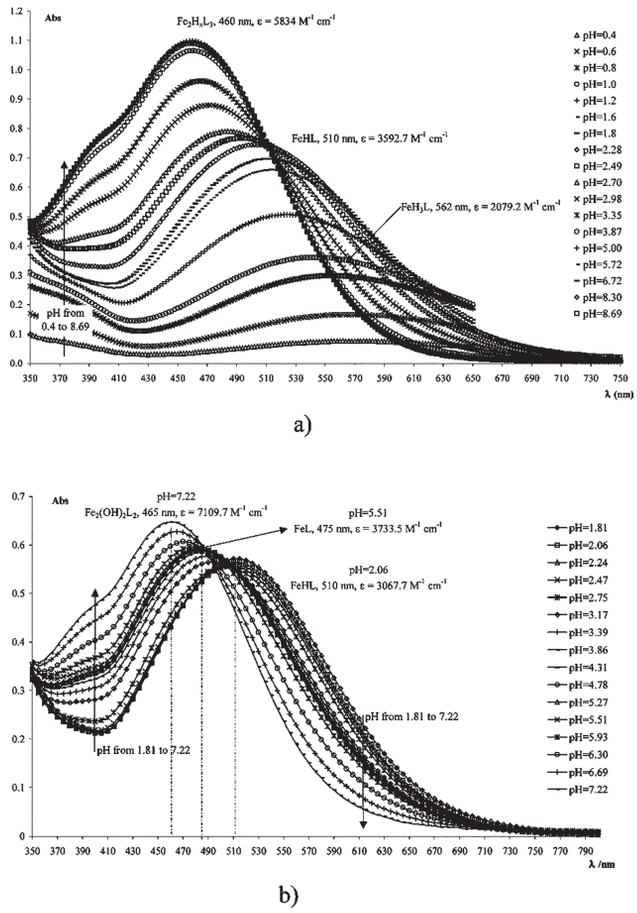

Fig. 3 Absorption spectra registered at various pH values for the Fe(III)–IDAPr(3,4-HP)$_2$ system at C_M = 1.99 × 10^{-4} M and two different metal-to-ligand molar ratios: 1 : 2 (a) and 1 : 1 (b).

coordination around each metal ion, despite eventual differences in the metal environment. For higher pH conditions, potentiometric measurements could be used to calculate the stability constants of other species, but holding constant the values previously determined by spectrophotometry.

Regarding the 1 : 2 stoichiometric conditions (Fig. 4(a)), above *ca.* pH 3.4 and up to *ca.* pH 9.1, another species starts being formed with λ_{max} gradually shifting to 460 nm (ε = 5460 M^{-1} cm^{-1}), a spectral characteristic of tris-chelated species, thus indicating the formation of 2 : 3 (M : L) dimeric species ($Fe_2H_xL_3$; x = 0–3). In this case, it can be assumed that one of the three ligand molecules could bridge two bis-chelated iron centers to complete their coordination sphere (Scheme 2(a)).

For the 1 : 1 stoichiometric conditions, analysis of the pH dependency of the absorption spectra (Fig. 4(b)) shows the existence of a bis-chelated species (λ_{max} = 510 nm) with maximum formation at *ca.* pH = 2.06 and it should correspond to the hydroxypyridinonate-to-iron CT band of the FeHL species. Above pH *ca.* 2.5 and up to pH 5.5 the amino group is expected to be deprotonated with formation of FeL. Comparison of its spectral parameters (λ_{max} = 475 nm, ε = 3734 M^{-1} cm^{-1}) with those of the previous species (FeHL) suggests the existence of some strengthening of the metal interaction; probably there is also formation of soluble mixed hydroxo species, FeHL(OH), instead of the assumed neutral FeL species, but they cannot be differentiated by potentiometry. Above this pH (pH 5.5–7.2) there is a further hypsochromic shift and absorbance increase of that band, which parallels the above referred one equivalent extra consumption of base in the potentiometric titration. This result suggests the formation of mixed hydroxo–ligand complexes which, according to the calculated spectral parameters (λ_{max} = 465 nm, ε = 7120 M^{-1} cm^{-1}, per complex), should be attributed to di-iron complex [$Fe_2(OH)_2L_2$].[24] Under this assumption, each iron centre would be coordinated by two hydroxypyridinone moieties of each ligand and one hydroxy

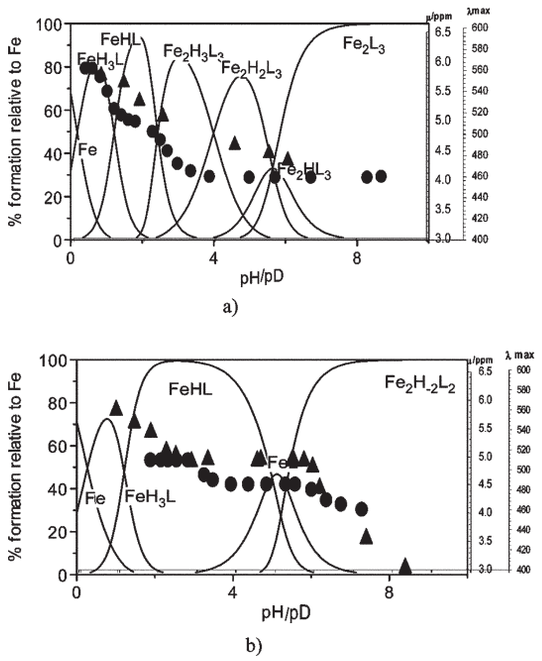

Fig. 4 Concentration distribution curves of the Fe-containing species for the system [Fe(III)–IDAPr(3,4-HP)$_2$] at 1:2 (M:L), $C_M = 2.844 \times 10^{-4}$ M) (a); and 1:1 (M:L), $C_M = 5.918 \times 10^{-4}$ M (b); at 25.0 °C, pH dependence of: λ_{max} of UV-Vis spectra of [Fe(III)–IDAPr(3,4-HP)$_2$] complexes, $I = 0.1$ M HNO_3 (▲); pD dependence of the molar magnetic moments (●).

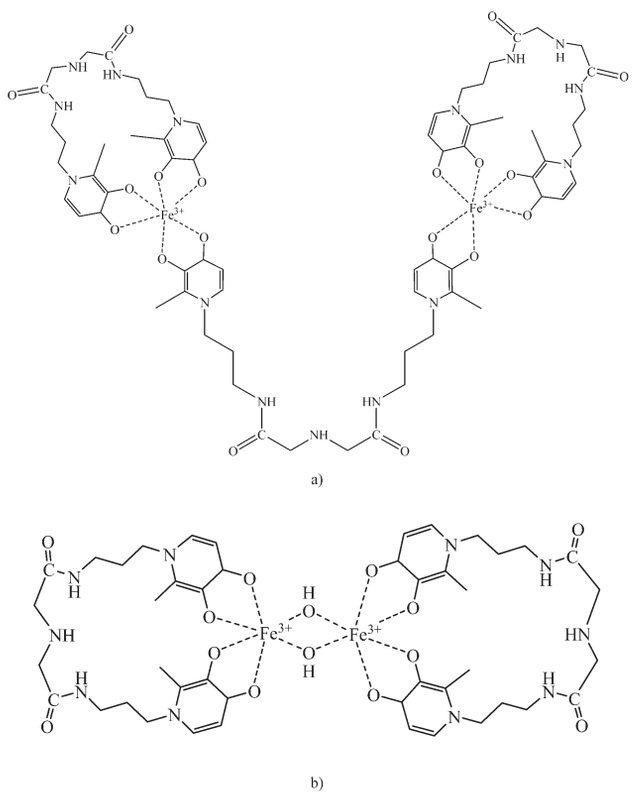

Scheme 2 Structural diagrams for the complexes: $Fe_2H_3L_3$ (a), $Fe_2(OH)_2L_2$ (b).

group (due to the hydrolysis of one water-coordinated molecule), but each one bridging the two metallic centers, according to Scheme 2(b). However, the presence of such μ_2-hydroxo bridged bonds in the core of dinuclear species is supposed to induce some distortion from the octahedral symmetry because the Fe–$O_{hydroxo}$ distances are expected to be shorter than those of Fe–O_{HP}.

Aiming at gain some light on the assumed equilibrium models the magnetic susceptibility was measured and the magnetic moment was calculated in about the same range of pH and conditions of the complexation studies. At $T = 298$ K, the pD dependence of the magnetic moment (μ_M) is illustrated in Fig. 4. For the 1:1 stoichiometry (Fig. 4(b)), at *ca.* pH 6 there is a large drop of μ_M (from *ca.* 5.0 to *ca.* 3.1 μ_B) which should result from a strong anti-ferromagnetic interaction between two Fe(III) sites, thus giving support to the assumed formation of a binuclear species with two bridging hydroxo groups. In fact, for *ca.* pH < 6, μ_M values are close to the magnetic moments reported for non-interacting mono-ferric complexes in the solid state (5.9 μ_B),[26] but for *ca.* pH ≥ 6 the value calculated for the magnetic moment (*ca.* 3.1 μ_B) is close to that found upon the formation of μ_2-oxo–diiron(III) complexes ($\mu_M = 3.4$ μ_B, at 300 K).[25] Concerning the 1:2 stoichiometric conditions, a steady decreasing of μ_M with the pH (for pH = 4, $\mu_M \approx 4.5$ μ_B) seems to parallel the formation of the dimeric species ($Fe_2H_iL_3$). Such behaviour can be attributed to a particular structure adopted by that complex, in which the metal centres are close enough to have some anti-ferromagnetic interaction and/or also the presence of diamagnetic impurities such as minor μ_2-hydroxo–diiron(III) species.

Since EPR spectra from the available apparatus require much higher concentrations and much lower temperatures than those used for potentiometric or magnetic moment measurements, with concomitant precipitation and changes on the speciation model, they could not be used to support the dimeric species.

Concerning the IDAPr(3,4-HP)$_2$–Al(III) and IDAPr(3,4-HP)$_2$–Ga(III) systems, analysis of their equilibrium models (Table 1 and Fig. 5) shows that, in agreement with the profiles of the potentiometric titration curves for the 1:1 stoichiometric conditions (Fig. 1), the hydrolytic processes for the aluminium system seem to parallel those for the ferric system, albeit, for the gallium system, they are present at a much lower extent. Since none of these Ga or Al complexes present d–d transitions or CT bands (and the ligand bands do not change too much upon complexation), the spectrophotometric techniques while used for the Ga complexation (low pH conditions) could not give any valuable help to support the models. Fortunately ^{27}Al NMR spectroscopy is usually able to discriminate between aluminium-coordinating modes, namely between octahedral ($\delta = -10$–40 ppm) and tetrahedral ($\delta = 60$–80 ppm).[27] Therefore ^{27}Al NMR spectra were obtained at the same concentration range used in potentiometry for the 1:1 (M:L) molar ratio, aimed at getting some clue to the geometry of the complexes. Two representative spectra recorded at two pD values and $T = 25$ °C are depicted in Fig. 6.

These spectra present a considerable amount of noise because ^{27}Al NMR spectrometry requires much higher concentrations than those used in potentiometry and increasing analytical concentration would affect the concentration distribution (the hydrolytic reactions could be reduced). Analysis of the spectra depicted in Fig. 6 shows, at very acidic conditions, the existence of a very sharp peak ($\delta = 0$ ppm), undoubtedly ascribed to the very symmetrical hexa-aqua octahedral complex $[Al(H_2O)_6]^{3+}$. All the remaining peaks are more or less broad and they should correspond to Al–L complex species. A further analysis of these spectra suggests that at *ca.* pH 2.5 the complexation has already started, with the formation of a complex species ($\delta = 66.7$ ppm), presumably with unsymmetrical tetrahedral geometry, and eventually slow exchange processes. According to the species distribution, they should be mainly ascribed to bis-chelated hydroxypyridinonate species.

The peak appearing at 39.2 ppm (*ca.* pH 5.57) should be attributed to a complex with octahedral geometry around the aluminium. Although this chemical shift is close to that reported for a tris-hydroxypyridonate coordination ($\delta = 37$ ppm, $W_{1/2} = 920$ Hz),[28] such a complete hydroxypyridinonate coordination cannot be considered for an Al-bis-hydroxypyridinone system at 1:1 metal-to-ligand molar ratio. However, these spectral data can be ascribed to an octahedral di-bridged di-(hydroxo-ligand–Al) $[Al_2(OH)_2L_2]$ complex, according to the proposed speciation model. Based on known chemical shifts

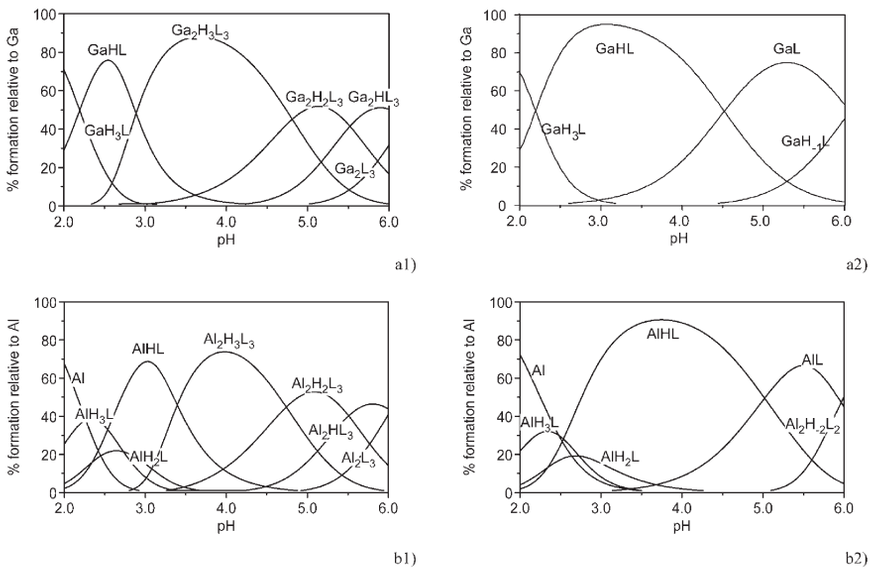

Fig. 5 Concentration distribution curves of the complexes formed for the systems Ga(III)–IDAPr(3,4-HP)$_2$ (a) and Al(III)–IDAPr(3,4-HP)$_2$ (b), at two different metal-to-ligand molar ratios (M : L): 1 : 2, $C_M = 2.844 \times 10^{-4}$ M (1) and 1 : 1, $C_M = 5.918 \times 10^{-4}$ M (2).

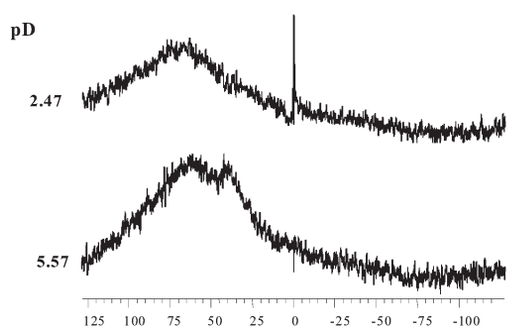

Fig. 6 ^{27}Al NMR spectra of [Al(III)–IDAPr(3,4-HP)$_2$] complexes at 1 : 1 metal-to-ligand molar ratio, $C_{Al} = 6.0 \times 10^{-4}$ M and indicated pD values.

for Al-coordination with three hydroxypyridinones (37 ppm) and four hydroxy groups (80.5 ppm), the contribution of two hydroxypyridinonates and one hydroxo group per aluminium centre could account for the observed chemical shift, thus supporting the proposed speciation model. Above *ca.* pH 6 there was precipitation under our experimental conditions and so no further spectra are obtained.

Regarding the Ga(III) complexation, the best fitting of the equilibrium data were obtained with the model suggested by UV-spectrophotometry titration at low pH and potentiometry for pH > 2, although for the Al(III) complexation a good model was obtained only based on the potentiometric data.

The rationalisation of those results is in good agreement with the speciation model listed in Table 1 and with the fact that the deprotonation of non-coordinated amino groups and coordinated water molecules can overlap. Furthermore, the studies on the complexation with these M^{3+} metal ions in aqueous solution, revealed a trend in the equilibrium constants, $\log\beta_{ML}$, for Al < Ga < Fe, which correlates well with the $\log K_{MOH}$ values reported for the same metal ions (11.27, 11.0, 8.47, respectively),[29] thus reflecting the rather ionic nature of this type of complexes, as previously reported for other hydroxypyridinone derivatives.[30]

Comparative analysis of complexation ability

Further conclusions about the metal-affinity of this chelator at physiological pH can be made based on the analysis of the calculated pM^{3+} values (which are directly related with the chelating strength) and comparison with the corresponding values for a set of usual synthetic and biological ligands presented in Table 1. It is clearly shown that, for the micromolar conditions that prevail in biological systems, IDAPr(3,4-HP)$_2$ presents a much higher metal chelating efficacy than the monohydroxypyridinone derivative, 3,4-DMHP (Deferriprone) (ΔpGa = 3.5). Thus, it can be predicted as a better scavenger for this type of hard metal ions then that drug. It also presents a higher chelating ability than the dihydroxypyridinonate analogue, KEMPPr(3,4-HP)$_2$,[11] which may due to the higher flexibility of the present ligand, the main motivation its design. Furthermore, IDAPr(3,4-HP)$_2$ shows a much higher chelating efficacy and specificity for these M^{3+} metal ions than some of the polyaminocarboxylate ligands with clinical applications (DPTA and DOTA).[31] The present ligand shows a chelating strength similar to that of DFB.[32,33] for this set of metal ions, albeit higher for millimolar concentrations.

Although from complexation data with transferrin (Table 1) it seems likely that IDAPr(3,4-HP)$_2$ and DFB can compete with apotransferrin for this set of metal ions,[34–36] the actual ability and mechanism of DFB to remove iron from transferrin remains unclear. However, since the monohydroxypyridinone Deferriprone proved to be able to mobilize iron from several iron-containing proteins, such as ferritin and transferrin,[37] an identical role, but with eventually higher efficacy, can be postulated for the present dihydroxypyridinone.

Molecular modelling

In order to get a further insight on the dimeric ferric complex structures of the present tetradentate ligand and better understanding of the magnetic properties presented by ferric solutions, brief molecular dynamics/mechanics calculations were performed to determine the most probable structure and the Fe–Fe distance for the $Fe_2H_{-2}L_2$ complex. We have used the CERIUS^2 program[38] with the default force-fields[39] and a previously reported approach,[40] based on the X-ray structure data for ferric complexes with the monohydroxypyridone 3,4-DMHP.[41] This modelling study (Fig. 7) helps in the elucidation of the structure, but it presents a shorter distance between the ferric centers (d_{Fe-Fe} = 2.75 Å) than that found in the literature for a series of μ_2-hydroxo–diiron(III) complexes (3.0–3.2 Å),[42] which could be mostly attributed to the force fields used in this brief simulation.

Distribution coefficient

The lipo/hydrophilic character of IDAPr(3,4-HP)$_2$ was evaluated based on its distribution coefficient ($\log D$) between 1-octanol and aqueous phase (Tris buffered at pH = 7.4). Although, at pH = 7.4, this compound is mainly in the neutral form, due to the low pK_a of the amino group, it is

Table 2 Biodistribution data in percent of injected dose per total organ (% I.D. ± SD) of ^{67}Ga–citrate (Group 1), ^{67}Ga–citrate with simultaneous intraperitoneal injection of IDAPr(3,4-HP)$_2$ (Group 2), ^{67}Ga–citrate with intraperitoneal injection of IDAPr(3,4-HP)$_2$ 30 min later (Group 3) and ^{67}Ga–IDAPr(3,4-HP)$_2$ (Group 4), 1 and 24 h after intravenous administration in female mice (n = 3–5)

	% I.D. ± SD							
	Group 1		Group 2		Group 3		Group 4	
Organ	1 h	24 h	1 h	24 h	1 h	24 h	1 h	24 h
Blood	3.2 ± 1.9	4.0 ± 2.0	3.1 ± 1.3	0.4 ± 0.1	3.0 ± 0.2	0.6 ± 0.2	1.3 ± 0.4	0.1 ± 0.01
Liver	1.8 ± 0.2	5.1 ± 1.9	1.8 ± 0.4	0.7 ± 0.1	1.2 ± 0.2	1.3 ± 0.3	0.5 ± 0.0	0.2 ± 0.1
Intestine	9.8 ± 1.6	4.3 ± 0.7	1.6 ± 0.2	1.0 ± 0.3	2.0 ± 0.4	1.0 ± 0.2	0.4 ± 0.0	0.2 ± 0.1
Spleen	0.1 ± 0.0	0.2 ± 0.1	0.2 ± 0.04	0.08 ± 0.0	0.1 ± 0.02	0.1 ± 0.0	0.02 ± 0.0	0.01 ± 0.0
Heart	0.1 ± 0.0	0.1 ± 0.0	0.2 ± 0.02	0.04 ± 0.0	0.1 ± 0.0	0.04 ± 0.0	0.03 ± 0.0	<0.01
Lung	0.3 ± 0.2	0.4 ± 0.1	0.5 ± 0.1	0.1 ± 0.0	0.3 ± 0.1	0.08 ± 0.0	0.1 ± 0.0	0.01 ± 0.0
Kidney	0.9 ± 0.1	1.3 ± 0.3	3.9 ± 1.0	1.0 ± 0.0	1.0 ± 0.2	1.0 ± 0.2	0.6 ± 0.1	0.3 ± 0.0
Muscle	11.3 ± 0.7	7.4 ± 0.8	5.2 ± 0.05	0.8 ± 0.2	4.0 ± 0.4	1.4 ± 0.2	2.5 ± 0.8	0.2 ± 0.1
Bone	17.1 ± 7.5	21.8 ± 3.2	2.3 ± 0.2	1.5 ± 0.2	2.5 ± 0.4	4.4 ± 1.0	1.2 ± 0.7	0.6 ± 0.3
Stomach	0.8 ± 0.3	0.5 ± 0.2	0.4 ± 0.0	0.2 ± 0.0	0.5 ± 0.2	0.2 ± 0.1	0.1 ± 0.0	0.04 ± 0.0
Excretion	17.2 ± 3.6	35.0 ± 7.2	78.4 ± 7.7	96.2 ± 0.4	71.3 ± 6.8	92.4 ± 1.0	76.0 ± 5.8	97.4 ± 0.6

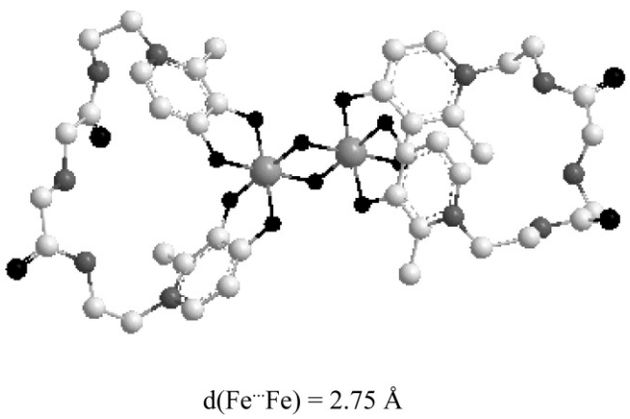

Fig. 7 Low-energy conformation simulated for the dimeric complex $Fe_2H_{-2}L_2$. For simplification of the picture, all the hydrogen atoms are removed.

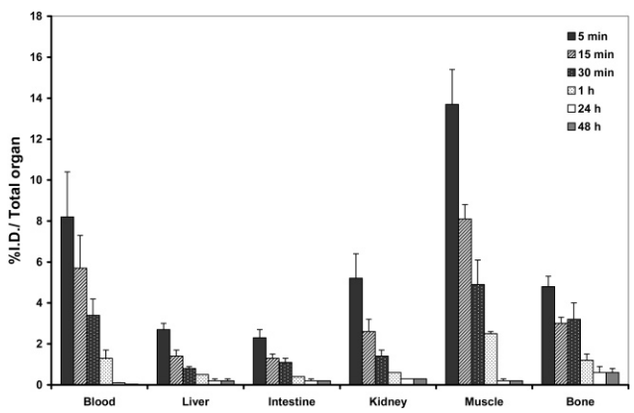

Fig. 8 Biodistribution data in most relevant organs, expressed as % I.D./total organ for ^{67}Ga–IDAPr(3,4-HP)$_2$ at 5 min, 15 min, 30 min, 1 h, 24 h and 48 h, after intravenous administration in female mice (n = 3–5).

more hydrophilic (log$D$ = −1.7 ± 0.02) than the corresponding monomeric species (log$D$ = −1.03, for 3,4-DMHP),[43] although slightly less then KEMPPr(3,4-HP)$_2$, which is negatively charged (log$D$ = −1.96 ± 0.02).[10] The high hydrophilic character of IDAPr(3,4-HP)$_2$ may be also due to existence of some hydrogen bonding between the amine group and the water molecules. Therefore, differences in target biological sites and clearance pathways are expected for these compounds.

Biological assays

In vivo assays were carried out in female mice to investigate both the biodistribution of the ^{67}Ga–IDAPr(3,4-HP)$_2$ complex and the efficacy of the chelating agent in the mobilisation of gallium in ^{67}Ga–citrate loaded mice, as models for other hard metal ions. The synthesis of the radioactive ^{67}Ga-complex with IDAPr(3,4-HP)$_2$ was accomplished with labelling efficiencies higher than 98%, as indicated by ITLC analysis. High radiochemical purity was obtained immediately after addition of the metal to the ligand solution at room temperature. Thus, 100 µL of a ^{67}Ga–IDA(Pr-3,4-HP)$_2$ solution, as equivalent to 0.5 µmol of ligand, were administered to each animal for biodistribution studies. Both the chelator and the ^{67}Ga-complex were well tolerated by animals at the administered doses with no obvious side effects. Tissue distribution data of radionuclide complex up to 48 h after administration, expressed as percentage of injected dose per total organ, can be overviewed in the histogram depicted in Fig. 8.

Biodistribution results show that the complex is quite efficiently cleared from the blood *via* both the hepatobiliar and renal pathways. Clearance from most organs including soft tissues like muscle, and bone is also quite rapid. Based on this biodistribution profile, radioactivity is mainly excreted from the whole animal body by the kidneys at a high rate (more than 75% in the first hour). ITLC analyses of mice urine samples, collected at sacrifice time, indicated that the radioactivity is mostly excreted as the ^{67}Ga complex. This observation demonstrates the high *in vivo* stability of this complex.

Therefore, this favourable biodistribution pattern (with a high rate of excretion and no significant uptake in any particular organ) as well as the high affinity of the ligand to coordinate these hard trivalent metal ions, suggested a good capability of the ligand to be potentially used to complex and remove *in vivo* overdoses of unwanted metal ions. To evaluate this ability two different experiments were carried out with the ^{67}Ga radiotracer. In a first set of animals, ^{67}Ga–citrate was intravenously administered immediately followed by intraperitoneal administration of 0.5 µmol of ligand in saline solution, while another set of animals were administered with the same solution of ligand only 30 min after the ^{67}Ga–citrate injection. Therefore biological distributions of the radiotracer in the presence or the absence of the ligand, at 1 h and 24 h, were compared (Table 4).

These biodistribution studies clearly evidence that the administration of the ligand highly interferes in the normal tissue distribution profile of the tracer leading to a rapid clearance from most tissues and a highly increased excretion rate of radioactivity from the animal body, as compared with the excretion of ^{67}Ga in the citrate form. Such enhancement is probably due to the higher metal-binding affinity of the ligand as compared to that of citrate (pGa = 18.8).[44] Comparative analysis of the biodistribution profiles of the radiotracer with administration of ligand solution, either simultaneously or 30 min later, *vs.* biodistribution of ^{67}Ga–IDAPr(3,4-HP)$_2$

demonstrates that there are no significant differences in the excretion rate. Clearance from most organs is always highly enhanced. However, at 1 h after administration of the ligand solution, there is a higher accumulation of activity in main organs such as blood and excretory organs when compared to that of the ^{67}Ga complex administration. These slight differences are probably due to some delay in the mobilisation of the metal.

The evidence that the administration of ligand solution induces a fastest elimination rate of ^{67}Ga from most tissues and whole animal body suggested its potential interest to be used *in vivo* to complex with trivalent metals that may be overdosed in some clinical situations. Comparison of our results with those found in the literature[45] for the ^{67}Ga complex with Deferriprone supports this hypothesis since a more rapid clearance and urinary excretion of the complex relative to the radiotracer were also found. To evaluate the *in vivo* behaviour and the ability of Deferriprone to coordinate *in vivo* with gallium in our animal model, a set of animal experiments were carried out by administration of ^{67}Ga citrate followed by intraperitoneal injection of 0.5 μmol of Deferriprone in saline solution and another group of animals were administered with the same amount of solution 30 min after administration of the radiotracer as we previously did with our ligand. Biodistribution was evaluated at 1, 24 and 48 h.

This preliminary study also indicated an increase in the excretion of the radiotracer when Deferriprone was administered (about 60.3 and 87.4% at 1 h and 48 h after administration, respectively). A comparative analysis of these results with data from our ligand is shown in the histogram of Fig. 9.

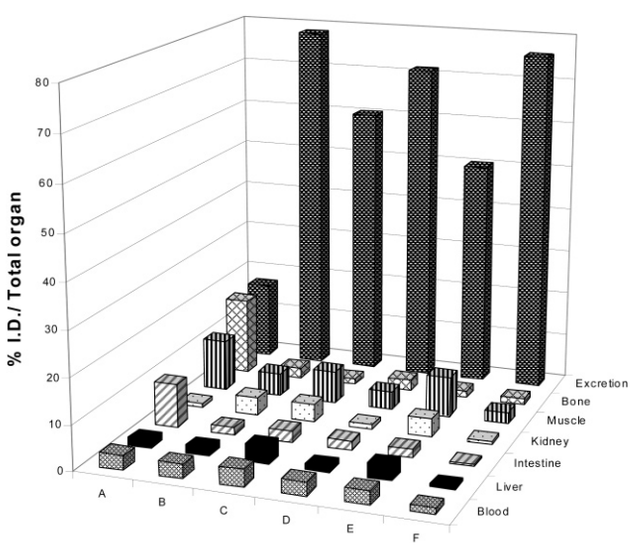

Fig. 9 Biodistribution data in percent of injected dose per total organ (% I.D. ± SD) of ^{67}Ga–citrate (A), ^{67}Ga–citrate with simultaneous intraperitoneal injection of IDAPr(3,4-HP)$_2$ (B) or Deferriprone (C), ^{67}Ga–citrate with intraperitoneal injection of IDAPr(3,4-HP)$_2$ (D) or Deferriprone (E) 30 min later; ^{67}Ga–IDAPr(3,4-HP)$_2$ (F), 1 h after intravenous administration in female mice (n = 3–5).

In this study it was found when IDA(Pr-3,4-HP)$_2$ was administered a more rapid clearance from organs and excretion of radioactivity was observed than in case of Deferriprone. Although the mechanism involved in the biodistribution in mice is not clear, namely the actual ability to mobilize gallium from transferrin, the present results support our expectations in terms of its high chelating capacity and allow us to suggest the potential usefulness of our compound for decorporating metals associated to pathologic situations.

Conclusions

A new dihydroxypyridinone derivative, IDAPr(3,4-HP)$_2$, having two 3-hydroxy-4-pyridinone (3,4-HP) chelating units attached to a iminodiacetic acid skeleton, has been prepared, studied in its complexation behaviour towards a set of hard metal ions and bio-assayed in mice. Equilibrium solution results demonstrate that, for a wide range of pH and the diluted conditions prevailing *in vivo*, this new compound possesses a higher efficacy for chelating hard metal ions (*e.g.* Fe^{3+}, Ga^{3+}, Al^{3+}) than the monohydroxypyridinone Deferriprone (a drug clinically used) and also some bioligands (*e.g.* citric acid and transferrin). Results of biological studies in mice indicated that the ^{67}Ga-complex is very stable *in vivo* without apparent toxicity and it presents a much more rapid clearance from most tissues than the citrate complex. As a gallium decorporating agent in mice it has also been proved to present a higher efficacy than Deferriprone. Therefore, independently of the mechanism involved in the *in vivo* gallium transfer and its dependence on other features than the favourable lipo/hydrophilic balance and the chelating strength, this set of results indicates there are good perspectives for this new compound to be a potential decorporating agent for this type of hard metal ions in overload situations without depletion of essential metal ions such as zinc.

Acknowledgements

The authors thank to the Portuguese Fundação para a Ciência e Tecnologia (FCT) (project POCTI/35344/00), the Hungarian Scientific Research Fund (OTKA) (OTKA T034674) and COST D21/001 program for financial support.

References

1 Z. D. Liu and R. C. Hider, *Med. Res. Rev.*, 2002, **22**, 26.
2 R. A. Yokel, *Coord. Chem. Rev.*, 2002, **228**, 97.
3 M. A. Santos, *Coord. Chem. Rev.*, 2002, **228**, 187.
4 G. J. Kontoghiorghes, *Lancet*, 1985, 817.
5 M. Meyer, J. R. Telford, S. M. Cohen, D. J. White, J. Xu and K. N. Raymond, *J. Am. Chem. Soc.*, 1997, **119**, 10093.
6 B. L. Rai, H. Khodr and R. C. Hider, *Tetrahedron*, 1999, **55**, 1129.
7 Y. Sun, M. J. Motekaitis and A. E. Martell, *Inorg. Chim. Acta*, 1998, **281**, 60.
8 A. J. Johnson, B. O'Sullivan and K. N. Raymond, *Inorg. Chem.*, 2000, **39**, 2652.
9 M. A. Santos, R. Grazina, L. Gano, S. Gama, *Port. Pat.*, PT102660, 2003.
10 M. A. Santos, R. Grazina, P. Buglyó, S. Gama and E. Farkas, *Polyhedron*, 2002, **21**, 2609.
11 M. A. Santos, R. Grazina, L. Gano and E. Farkas, unpublished work.
12 *Purification of Laboratory Chemicals*, ed. W. L. F. Armarego and D. D. Perrin, Butterworth-Heinemann Press, Oxford, 4th edn., 1999.
13 F. J. C. Rossotti and H. Rossotti, *J. Chem. Educ.*, 1965, **42**, 375.
14 P. Gans, A. Sabatini and A. Vacca, *Talanta*, 1996, **43**, 1739.
15 A. Sabatini, A. Vacca and P. Gans, *Talanta*, 1974, **21**, 53.
16 L. Zékány and I. Nagypál, in *Computational Methods for the Determination of Stability Constants*, ed. D. Leggett, Plenum Press, New York, 1985.
17 M. A. Santos, R. Grazina, A. Q. Neto, G. Cantinho, L. Gano and L. Patrício, *J. Inorg. Biochem.*, 2000, **78**, 303.
18 A. Leo, C. Hansch and D. Elkins, *Chem. Rev.*, 1971, **71**, 526.
19 A. K. Covington, M. Paabo, R. A. Robinson and R. G. Bates, *Anal. Chem.*, 1968, **40**, 700.
20 D. F. Evans, *J. Chem. Soc.*, 1959, 2003.
21 E. N. Sloth and C. S. Garner, *J. Chem. Phys.*, 1954, **22**, 2064.
22 E. T. Clarke and A. E. Martell, *Inorg. Chim. Acta*, 1992, **191**, 57.
23 R. Karlicek and J. Majer, *Collect. Czech. Chem. Commun.*, 1972, **37**, 151.
24 T. Justel, M. Muller, T. Weyhermuller, C. Kressel, E. Bill, P. Hildebrandt, M. Lengen, M. Grodzicki, A. X. Trautwein, B. Nuber and K. Wieghardt, *Chem. Eur. J.*, 1999, **5**, 793.
25 M. Gerloch, J. Lewis, F. E. Mabbs and A. Richards, *J. Chem. Soc. A*, 1968, 112.
26 W. H. Armstrong, M. E. Roth and S. J. Lippard, *J. Am. Chem. Soc.*, 1987, **109**, 6318.
27 F. R. Venema, J. A. Peters and H. van Bekkum, *J. Chem. Soc., Dalton Trans.*, 1990, 2137.
28 L. Simpson, S. J. Rettig, J. Trotter and C. Orvig, *Can. J. Chem.*, 1991, **69**, 893.

29 A. E. Martell and R. M. Smith, *Critical Stability Constants*, Plenum Press, New York, 1989, First Supplement, pp. 428–429.
30 M. A. Santos, M. Gil, S. Marques, L. Gano, G. Cantinho and S. Chaves, *J. Inorg. Biochem.*, 2002, **92**, 43.
31 *Critically Selected Stability Constants of Metal Complexes Database*, ed. A. E. Martell, R. M. Smith and R. J. Motekaitis, College Station TX, Version 4.0, 1997.
32 B. J. Hernlem, L. M. Vane and G. D. Sayles, *Inorg. Chim, Acta*, 1996, **244**, 179.
33 E. A. Enyedy, I. Pocsi and E. Farkas, unpublished results.
34 R. J. Motekaitis and A. E. Martell, *Inorg. Chim. Acta*, 1991, **183**, 71.
35 H. R. Harris and V. L. Pecoraro, *Biochemistry*, 1983, **22**, 292.
36 W. R. Harris and J. Sheldon, *Inorg. Chem.*, 1990, **29**, 119.
37 G. Faa and G. Crisponi, *Coord. Chem. Rev.*, 1999, **184**, 291.
38 *CERIUS*^{2} *Program*, Version 3.0, 1998, Molecular Simulation Inc., Cambridge.
39 A. K. Rappe, C. J. Casewit, K. S. Colwell, W. A. Goddard and W. M. Skiff, *J. Am. Chem. Soc.*, 1992, **114**, 10024.
40 M. A. Esteves, M. C. T. Vaz, M. L. S. Gonçalves, E. Farkas and M. A. Santos, *J. Chem. Soc., Dalton Trans.*, 1995, 2565.
41 E. T. Clarke, A. E. Martell and J. Reibenspies, *Inorg. Chim. Acta*, 1992, **196**, 177.
42 S. M. Gorun and S. J. Lippard, *Inorg. Chem.*, 1991, **30**, 1625.
43 R. A. Yokel, A. K. Datta and E. G. Jackson, *J. Pharmacol. Exp. Ther.*, 1991, **257**, 100.
44 A. E. Martell and R. M. Smith, *Critical Stability Constants*, Plenum Press, New York, 1977, vol. 3, p. 161.
45 D. A. Clevette, D. M. Lyster, W. O. Nelson, T. Rihela, G. A. Webb and C. Orvig, *Inorg. Chem.*, 1990, **29**, 667.